

AN ABSTRACT OF THE THESIS OF

Luke A. Scoggins for the degree of Master of Science in Civil Engineering presented on June 22, 2007.

Title: 3-D Finite Element Modeling in OpenSees for Bridge Live-Load Girder Distribution Factors.

Abstract approved:

Michael H. Scott

A generalized, three-dimensional, finite element bridge model was created in order to efficiently and accurately assess live-load girder distribution factors for a variety of bridge types. This model shortens the time required by bridge analysts to develop individual finite element models for bridges of varying geometries. The creation of the generalized bridge model was based on previous modeling techniques successfully implemented and tested by different researchers. The proposed modeling scheme utilizes a combination of shell elements for the deck, frame elements for the girders, and rigid beam links connecting these two element types. The versatility of the finite element program, *OpenSees*, allowed for the creation of this generalized bridge model. The Tcl scripting language, used to define the analysis for implementation in *OpenSees*, enhances the capabilities of generalizing the truck types and loading procedures for analysis.

The generalized finite element bridge model developed for use in *OpenSees* was validated through comparison to two bridges analyzed by field testing and finite element modeling in a previous research study. The girder distribution factors of these

conventionally reinforced concrete bridges were determined with the generalized bridge model and compared to the results of the previous research and to factors determined with the AASHTO LRFD (2003) specification. The results determined with the generalized model compared well with the results of the previous study and effectively validated the model. Factors evaluated with AASHTO LRFD (2003) were shown to be generally conservative. The generalized bridge model was found to accurately and efficiently evaluate live-load girder distribution factors and could prove useful to economically rate a large number of bridges.

©Copyright by Luke A. Scoggins
June 22, 2007
All Rights Reserved

3-D Finite Element Modeling in OpenSees for Bridge
Live-Load Girder Distribution Factors

by

Luke A. Scoggins

A THESIS

submitted to

Oregon State University

in partial fulfillment of
the requirements for the
degree of

Master of Science

Presented June 22, 2007

Commencement June 2008

Master of Science thesis of Luke A. Scoggins presented on June 22, 2007.

APPROVED:

Major Professor, representing Civil Engineering

Head of the School of Civil and Construction Engineering

Dean of the Graduate School

I understand that my thesis will become part of the permanent collection of Oregon State University libraries. My signature below authorizes release of my thesis to any reader upon request.

Luke A. Scoggins, Author

ACKNOWLEDGEMENTS

The author expresses sincere appreciation for the guidance and assistance of Dr. Michael Scott throughout the entire project. Also, in assisting with the comprehension of bridge construction and behavior, Dr. Chris Higgins' help and patience was unabated and much appreciated. The inherent contribution from the great minds of the surrounding graduate students in the CCE department at OSU was invaluable. And a special thanks to Oregon Department of Transportation for making this project possible.

CONTRIBUTION OF AUTHORS

Dr. Michael H. Scott assisted with the technical and theoretical aspects of this project, and was especially insightful with the interpretation of the Tcl language and the *OpenSees* program. Dr. Christopher Higgins provided modeling advice through discussions of conventionally reinforced concrete bridge composition and behavior. He also helped with the interpretation of results from the Potisuk and Higgins (2007) paper.

TABLE OF CONTENTS

	<u>Page</u>
Chapter 1: General Introduction.....	1
Chapter 2: Creation of a Generalized 3-D Finite Element Bridge Model.....	3
Objective	3
Discussion of Model	4
Load Modeling.....	7
Model Setup	9
Variable Definition.....	13
Model Verification.....	15
Summary	18
References	19
Chapter 3: Validation of a Generalized 3-D Finite Element Bridge Model	21
Objective	21
Description of Bridges	21
Field Testing/Previous Analysis	24
Model Setup	26
Model Validation/Comparison.....	28
Controlling Distribution Factors	31
Summary	35
References	37
Chapter 4: General Conclusions.....	38
Appendices.....	39
Appendix A: Tcl Input for the Willamette River Bridge	40

LIST OF FIGURES

<u>Figure</u>	<u>Page</u>
2.1 Diagram of rigid link connection.	7
2.2 Diagram of standard AASHTO HS-20 design truck loading.....	7
2.3 Geometry for load distribution at a single node.....	11
2.4 Consistent nodal loads procedure.....	11
2.5 Diagram of bridge components and Tcl variables for user entry.....	14
2.6 Two span continuous beam structure for model verification.....	17
2.7 Convergence of the summed reaction of bridge girders.	17
3.1 Willamette River Bridge layout (all units in millimeters).	23
3.2 McKenzie River Bridge layout (all units in millimeters).	24
3.3 FE bridge models with caption of applied boundary conditions.....	28

LIST OF TABLES

<u>Table</u>	<u>Page</u>
3.1 Summary of results from Potisuk & Higgins (2007).	26
3.2 Shear GDF comparison with Potisuk & Higgins (2007) FE analysis.	30
3.3 Generalized FEM girder distribution factors.	33
3.4 Controlling girder distribution factor comparison	34

DEDICATION

To my wife, Kristen, for her unending patience and encouragement, and to my parents for their constant support throughout school and for instilling in me the value of learning and contemplation. Thank you.

Chapter 1: General Introduction

The determination of the distribution of live-load to bridge girders is a necessary step in order to rate a bridge based on its response to loadings which simulate vehicles moving across the deck. Different vehicle types combined with the numerous possible locations for these vehicles on the bridge deck leads to a difficult and time consuming analysis. For this reason, the AASHTO LRFD Bridge Design Specification (2003) contains equations which simplify the determination of live-load girder distribution factors. These equations are based on standard bridge properties that have the most significant affect on load distribution. They were formulated from research for the National Cooperative Highway Research Program 12-26 project (Zokaie et al. 1991). This research extended the use of the distribution factor equations by encompassing a wide range of bridge types and geometries. Because of the large variance in bridge types and geometries, the AASHTO LRFD equations have a tendency to be overly conservative for certain bridge geometries (Barr 2006). Also, if bridge geometry varies greatly along the span, the equations may become inapplicable (Zokaie 2000).

When a more accurate analysis of the girder distribution factors is required or when the use of the AASHTO LRFD equations is restricted, it is advised to use a grillage or detailed analysis by the finite element method (Zokaie 2000). A finite element analysis can take time to develop and test for accuracy of its results. An analyst often creates each model for a specific bridge by assigning the appropriate constitutive properties, geometry and boundary conditions to represent the actual behavior of the system. The analyst must also select proper element types for the model to ensure accurate

simulation of the structural components. Separately, a loading procedure that envelops the maximum loading the bridge is likely to sustain during its lifetime must be applied in order to obtain realistic live-load girder distribution factors.

The extensive variability of each FE model causes the analyses to be lengthy and expensive when applied to an assortment of bridges for a comparison study or general bridge evaluations. A generalized FEM that encompasses a wide range of bridge geometries would be useful in reducing the amount of time it takes the analyst to develop a model for each bridge analysis. Additionally, a shorter run time for each model will further reduce the total time allotted to the analyses.

Chapter 2: Creation of a Generalized 3-D Finite Element Bridge Model

Objective

The objective of this paper is to develop a generalized finite element model to determine live-load girder distribution factors for an assortment of bridges. The modeling approach will provide enough versatility to encompass a wide range of bridges through the entry of a limited number of variables required to define each bridge. These variables define the geometric and constitutive properties of a bridge as well as the loading procedure for each analysis. The short time required to define and analyze each bridge is central to efficient rating and assessment.

The creation of a generalized model that is adaptable to a large range of bridge types with different loading procedures requires a versatile finite element program. For this reason, the FE program *OpenSees* was used to develop the generalized bridge model. This program was developed for the research community for analyzing structures subject to dynamic earthquake loads and extends the Tcl scripting language to support commands to define the geometry, loading, formulation and solution of the model. The analyst can implement variables, mathematical expressions, control structures, procedures, and file manipulation during the creation of the Tcl script which is used to run the FE program (Mazzoni et al. 2006). This setup allows for a highly adaptable model based on the intricacies of the Tcl language and provides the necessary platform for the generalized bridge model subject to various moving loads.

Discussion of Model

There are a number of different finite element modeling techniques applicable to a bridge analysis. Basic considerations for every model are element types and the constitutive properties depending on either a linear or nonlinear material behavior. The creation of the generalized model requires simplicity in setup and a reduced analysis time. The modeling parameters are selected with these considerations at the forefront.

A number of researchers have successfully developed and tested bridge models of existing structures. These models, operating in the elastic range, were shown to accurately predict the behavior of existing bridges at the service level. For these analyses, element types are used in combination with the linear-elastic assumption to determine live-load distribution for various bridge types. Mabsout et al. (2004) modeled an existing reinforced concrete slab bridge using quadrilateral shell elements in order to study wheel load distribution. The results were successfully compared to field measurements. Potisuk and Higgins (2007) studied shear distribution in conventionally reinforced concrete bridges by comparing field measurements to a finite element model using 8-node shell elements for the deck, girders, diaphragms, and bent caps and frame elements for the columns. Hughs and Idriss (2006) modeled a prestressed concrete box girder bridge using shell elements for the deck and frame elements for the girders. The two element types were connected by rigid beam links to achieve composite action. Barr et al. (2001) employed the same modeling scheme as Hughs and Idriss (2006) for skewed prestressed concrete girder bridges. Tabsh and

Tabatabai (2001) considered live-load distribution of oversized trucks on composite steel girder bridges with concrete decks. Their model employed beam elements for the flanges of the girders and also for the bridge diaphragms. The girder webs and bridge deck were modeled with 4-node shell elements. Rigid beam elements were used to connect the top flange of the girders to the shell elements of the deck. Barr et al. (2006) compared three different finite element modeling techniques: shell elements for the entire structure, rigid beam links connecting shell elements for the deck and frame elements for the girders, and rigid beam links connecting solid elements for the deck and frame elements for the girders. All three modeling schemes produced similar results and were within 4% of actual bridge measurements. Chung and Sotelino (2005) used shell elements to model a concrete deck over steel girders. The girders were modeled with various techniques for comparison. The web and flanges of each girder were modeled with different combinations of beam and shell elements. They found that accurate results were achieved with the most economic model using simple beam elements for the girders with rigid links connecting them to the shell elements of the deck.

Considering all these previous works for the creation of an efficient generalized bridge model, a linear-elastic analysis was assumed. Therefore, iteration of the stiffness matrix is not required upon each load application and analysis time is considerably less compared to a nonlinear or inelastic model. The model, through assignment of constitutive properties, reserves the ability to analyze bridges composed of various

materials; the focus of this paper is to construct a bridge model adapted to reinforced concrete, but the linear-elastic assumption can be extended to other materials. The modeling of concrete without consideration of cracking was shown to have little adverse effect on the overall behavior of the bridge system within the elastic range of the structure (AASHTO LRFD 2003).

To further reduce analysis time, the degrees of freedom of the model are kept to a minimum through the selection of appropriate elements. For this reason, 4-node shell elements are used to model the deck of the generalized bridge model. Frame elements are used to model the girders, diaphragms, and bent caps. Rigid beam links are used between the deck nodes and the girder, diaphragm, and bent cap nodes to enforce composite action. This modeling scheme, shown in Fig. 2.1, was chosen both because it has fewer degrees of freedom and it is easier to implement than a model using either shell elements for the entire structure or using solid elements for the deck in place of the shell elements.

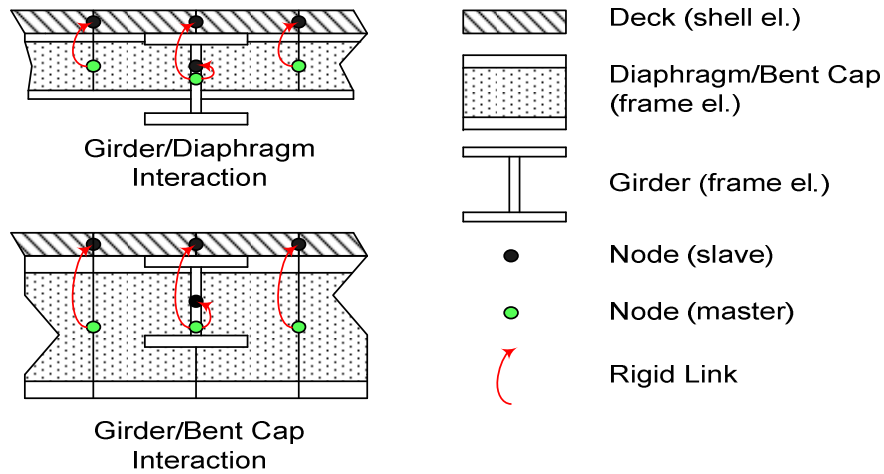


Fig. 2.1: Diagram of rigid link connection.

Load Modeling

To determine live-load girder distribution factors, an AASHTO HS-20 truck is commonly used as per AASHTO specifications (2003) and is shown in Fig. 2.2. A few different loading techniques have been used by researchers to apply this standard truck loading.

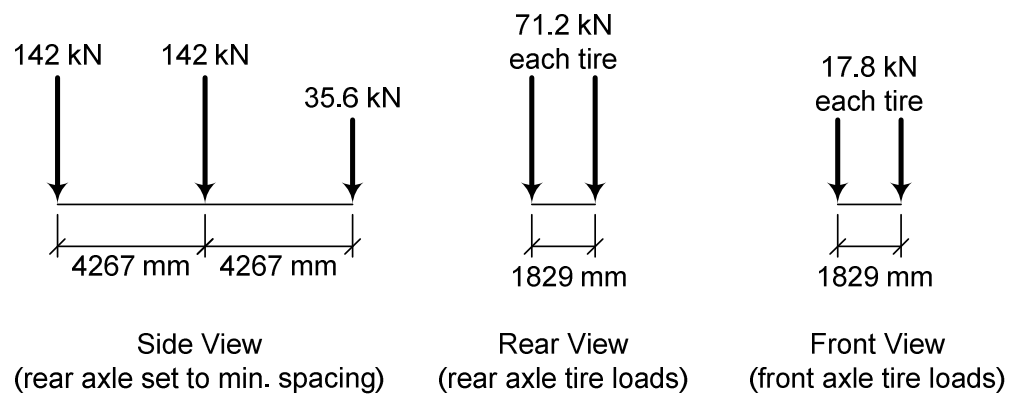


Fig. 2.2: Diagram of standard AASHTO HS-20 design truck loading.

Most often, influence lines are used to determine the longitudinal locations of interest on the bridge span where the magnitude of the shear or bending stress is at a maximum. Barr et al. (2006) used influence lines to find these critical longitudinal locations and then applied an HS-20 truck at these locations and systematically moved the truck across the width. Tabsh and Tabatabai (2001) used the same technique. Potisuk and Higgins (2007) developed a three-dimensional shear influence surface for a specified location of both interior and exterior girders. The magnitude of the HS-20 truck tire loads were then multiplied by the influence ordinates to find the maximum value of shear for the girder section. All three cases use the following method to determine the distribution factors: the maximum stress or force is found in the girder and divided by the sum of the stresses or forces in all girders at the section of interest; this value is then multiplied by the numbers of lanes loaded and by the multi-presence factor as listed in the AASHTO LRFD (2003) specification. The equation is described as

$$\text{GDF} = \frac{N \gamma f_m}{\sum_{i=1}^n f_i} \quad (\text{Equation 2.1})$$

where N=number of lanes loaded; γ =multiple presence factor (1.2 for N=1; 1.0 for N=2); f_m =maximum girder response (requisite response for shear or moment);

$\sum_{i=1}^n f_i$ =sum of response of all girders at the associated cross-section.

The adaptability of the Tcl script allowed for the definition of various loadings. The generalized model was developed in such a way as to allow the user to define both longitudinal and transverse sections of interest for the systematic application of the truck load at specified increments. This allows for the analyst to choose either a localized area of interest based on influence lines, or to apply truck loading to the entire bridge and bypass the process of developing influence lines. Also, a separate loading procedure allows for influence surfaces to be created by applying a point load to all deck nodes. The analyst chooses the locations of interest for these surfaces.

Model Setup

The previously determined modeling technique and loading procedure were implemented in *OpenSees* through the creation of a Tcl script. *OpenSees* possesses a quadrilateral ShellMITC4 element which was used to model the deck. The element uses a bilinear isoparametric formulation with a modified shear interpolation which improves thin-plate bending performance (Bathe et al. 2000) and allows for the use of larger elements with a set thickness. This element was selected because it is the only available shell element in *OpenSees*. The advantages of using such an element are not fully realized for this application.

Forces cannot be applied directly to the body of these shell elements. To apply truck loads to any location on the surface of the deck, a consistent nodal loads procedure was implemented in Tcl to evenly distribute these body forces to the nodes of each

element; modification of the *OpenSees* source code is avoided with implementation of this Tcl procedure. Typically, element shape functions, also interpolation functions in most FE texts, are used for this force distribution. For the 4-node shells, this requires the solution of simultaneous equations each time a body force is applied to the shell element. Although this can easily be implemented within the Tcl script, to increase computational efficiency, a different approach was assumed which avoids the solution of simultaneous equations. The adopted procedure is based on standard trigonometric equations. The load location is projected to each side of the element and the enclosed area, adjacent to each node, is determined. This area is divided by the entire element area, multiplied by the body force and then applied to the node diagonally opposite the original node. Fig. 2.3 shows this distribution for a node and Fig. 2.4 shows the entire Tcl procedure which utilizes a nodal lookup for each selected element number. The element number subject to the applied load is previously determined in the Tcl script from global coordinates of the loads and elements.

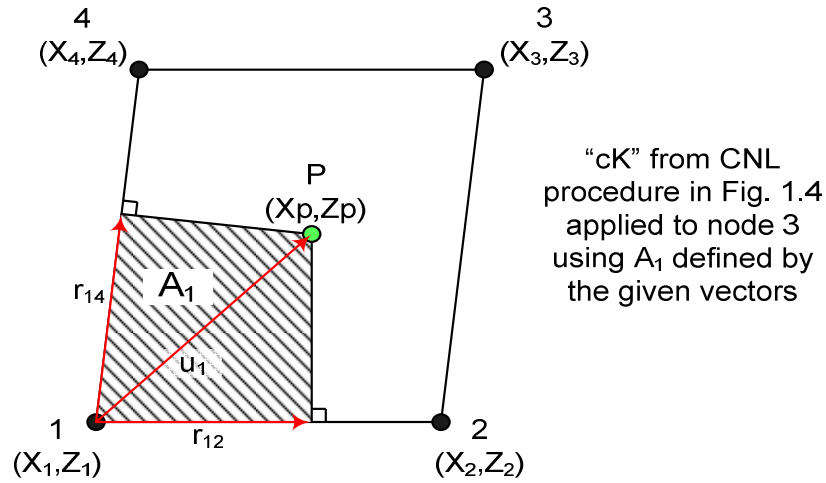


Fig. 2.3: Geometry for load distribution at a single node.

```

proc Cnl {elem Xp Zp} {
set nodes [eleNodes $elem]
set j 1
foreach node $nodes {
set X($j) [nodeCoord $node X]
set Z($j) [nodeCoord $node Z]
incr j
}
foreach {i j} {1 2 2 3 3 4 4 1} {
set rv($i,$j) [expr abs((($Xp-$X($i))*($X($j)-$X($i)))+(($Zp-$Z($i))*($Z($j)-$Z($i))))]
set rv($j,$i) [expr abs((($Xp-$X($j))*($X($i)-$X($j)))+(($Zp-$Z($j))*($Z($i)-$Z($j))))]
set v($i,$j) [expr pow((($X($j)-$X($i)),2)+pow((($Z($j)-$Z($i)),2),2)]
set v($j,$i) [expr pow((($X($i)-$X($j)),2)+pow((($Z($i)-$Z($j)),2),2)]
set vxu($i,$j) [expr abs((($X($j)-$X($i))*($Zp-$Z($i)))-(($Z($j)-$Z($i))*($Xp-$X($i))))]
set vxu($j,$i) [expr abs((($X($i)-$X($j))*($Zp-$Z($j)))-(($Z($i)-$Z($j))*($Xp-$X($j))))]
}
foreach {i j k} {1 2 4 2 3 1 3 4 2 4 1 3} {
set A$i [expr
(($rv($i,$j)/$v($i,$j))*$vxu($i,$j))+(($rv($i,$k)/$v($i,$k))*$vxu($i,$k))/2]
}
set Atot [expr $A1+$A2+$A3+$A4]
set cI [expr $A3/$Atot]
set cJ [expr $A4/$Atot]
set cK [expr $A1/$Atot]
set cL [expr $A2/$Atot]
return "$cI $cJ $cK $cL" ;# Fraction of Load Contribution to Nodes
}

```

Fig. 2.4: Consistent nodal loads procedure.

The girders, diaphragms and bent caps are modeled with force-based formulated frame elements with six degrees of freedom. The advantages of this nonlinear element are not fully realized for an elastic analysis, but it is the best available element in *OpenSees* which reserves the ability to record shear and moment forces directly at any integration point where, for the bridge model, a linear-elastic constitutive model is assumed. This feature is invaluable to efficiently post-process the data. Also, variations of section dimensions, as with tapered or haunched girders, can be captured through definition of the geometric properties of the element at each integration point within a single element. This alleviates the need to discretize the girder elements to fully incorporate the geometric variation of a taper or haunch. The savings in discretization is also observed in the shell elements as the lengths of the girder elements are synonymous with the dimensions of the shell elements along the plane of interest. That is, girder element lengths are equivalent to shell element longitudinal width; diaphragm and bent cap element lengths are equal to shell element transverse width. This ensures the nodes of the frame elements and those of the shell elements are on equal planes for proper connectivity. Fig. 2.1 shows an example of this in the transverse direction.

To connect the different element types, rigid beam links are used to ensure composite action of the deck, girders and diaphragms, or bents. The connection of these links is defined by a master node and a slave node. The displacement of the slave node is constrained to that of the master node. The assignment of either node as master or

slave is inconsequential in terms of system behavior except that an otherwise restrained node must be assigned as a master node. All deck nodes are designated slave nodes; girder and diaphragm nodes are designated master nodes except at the intersection of the girders and diaphragms or bent caps. At the intersection of the diaphragm and girder, the girder node acts as the master and the diaphragm node is a slave. This ensures proper restraints on the girders as is commonly required at a bridge abutment where the supports are at the girder line. At intersections of the girders and the column supported bent caps, the node of the bent cap is assigned as the master. Refer to Fig. 2.1 for the rigid link details at these interaction locations.

Variable Definition

The generalized bridge model was encapsulated in a Tcl script and setup such that only a few variables, specific to each bridge, are required to be entered by the analyst. The entire bridge model is defined by these variables. They include the following: girder and diaphragm dimensions, deck thickness, span lengths, girder spacing at bridge ends and main spans, location of diaphragms, skew angle, overhang distance, and girder and deck constitutive properties. Fig. 2.5 shows some of the common bridge components and details of the variables; App. A displays the variables within the Tcl script.

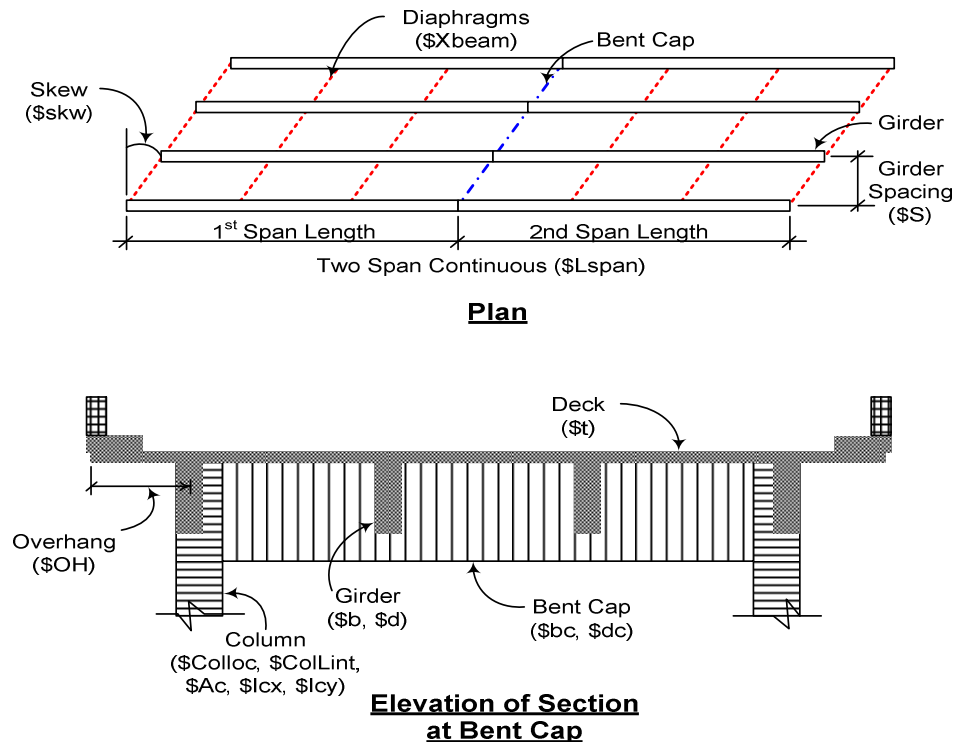


Fig. 2.5: Diagram of bridge components and Tcl variables for user entry.

The longitudinal length of each element must be specified along with the number of divisions of the shell elements between girders and on the overhangs. This allows for simple discretization of the model. Also, the analyst defines the loading scenario by setting the variables which define the truck type. For example, variables such as longitudinal and horizontal spacing between the tires of the truck and the magnitude of each tire load allow the user to specify an HS-20 or other design truck. In conjunction, the analyst assigns the number of trucks to apply and the spacing between them. The analyst also reserves the ability to set the section of interest for the load application.

Alternative to specifying truck loadings, the analyst can set elements of interest and create influence surface plots.

The creation of the surface plots and values for the girder distribution factors requires some post-processing. *OpenSees* contains an assortment of recorder objects which can be set to monitor various items of interest during an analysis. The post-processing is achieved with the use of the Tcl language by writing to a *Matlab* compatible file for evaluation of the bridge analysis.

Model Verification

To verify the accuracy of the generalized model, a convergence study was performed. A two span continuous reinforced concrete bridge was selected with arbitrary girder dimensions and span lengths. The bridge had span lengths of 15.2 m (50 ft) with four girders spaced 2.4 m (8.33 ft). Diaphragms were located at quarter points of each span. The deck was 152 mm (6 in) thick and did not overhang beyond the exterior girders. The girders, diaphragms, bent caps were all 1219 mm (48 in) deep and 305 mm (12 in) wide. An elastic modulus of 27.6 GPa (4000 ksi) was used with a Poisson's ratio of 0.2. The bridge was analyzed with five different longitudinal element lengths of 152, 305, 406, 610, 813, and 1219 mm (6, 12, 16, 24, 32, and 48 in, respectively). The shell elements modeling the deck were equally divided to assume similar shell element lengths in the horizontal direction. In the same order of the stated element lengths, the number of shell elements associated with each model are 9600, 2496, 1440, 672, 360,

and 192; the number of beam elements in each model are 1232, 632, 482, 332, 241, and 182, respectively.

To verify the model, a 61.78 kN/m (13.88 k/ft) line load was evenly distributed across the full width of the deck at the middle of the first span. The vertical reactions at the near side supports were recorded and summed together in order to compare the reaction to a closed-form solution of a two-dimensional two span continuous beam with an equivalent 444.8 kN (100 k) point load applied at the middle of the first span. The closed-form support reactions were determined from standard structural analysis techniques for a two-span continuous prismatic beam where the reaction at the end support of the first span is evaluated as $13/32$ of the applied load. The closed-form solution is shown in Fig. 2.6 with the applied loading and support reactions. This initial load was removed and a subsequent load, equal in magnitude, was applied at the center of the second span in order to compare the time required for the application of additional loads. The second applied load serves to simulate subsequent truck loads applied to the model which do not require the formulation and solution of the stiffness matrix as is required with the first applied load. For each of the two applied load cases the time is set relative to the bridge model composed of 1219 mm (48 in) elements. Plots of the convergence study and the relative time associated with each analysis are shown in Fig. 2.7. The values from the finite element analysis do not converge exactly to the closed-form solution. The three-dimensional finite element model may transfer load differently due to transverse bending and different support conditions with

restraints located only at girders and not across the entire cross-section. From the study, it was determined that an element length between 610 mm (24 in) and 305 mm (12 in) will produce valid results. The elapsed time of an analysis for an element length of 152 mm (6 in) is much too large to justify further discretization of the model.

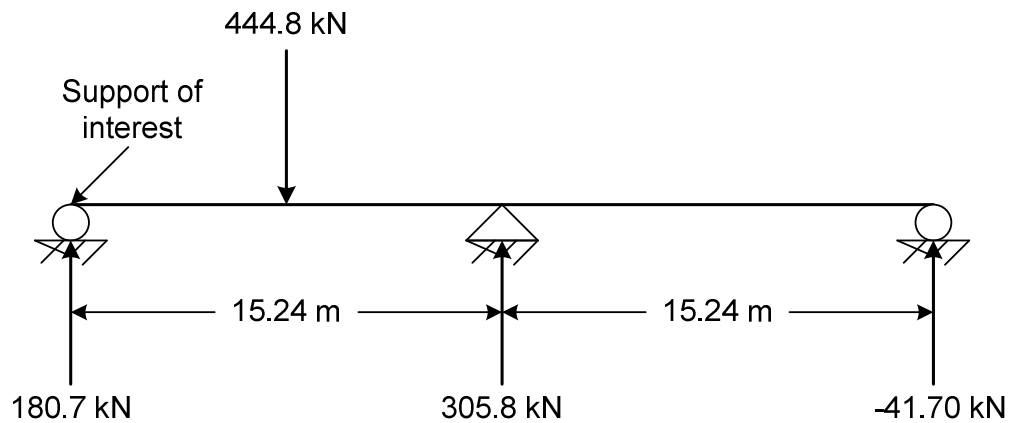


Fig. 2.6: Two span continuous beam structure for model verification.

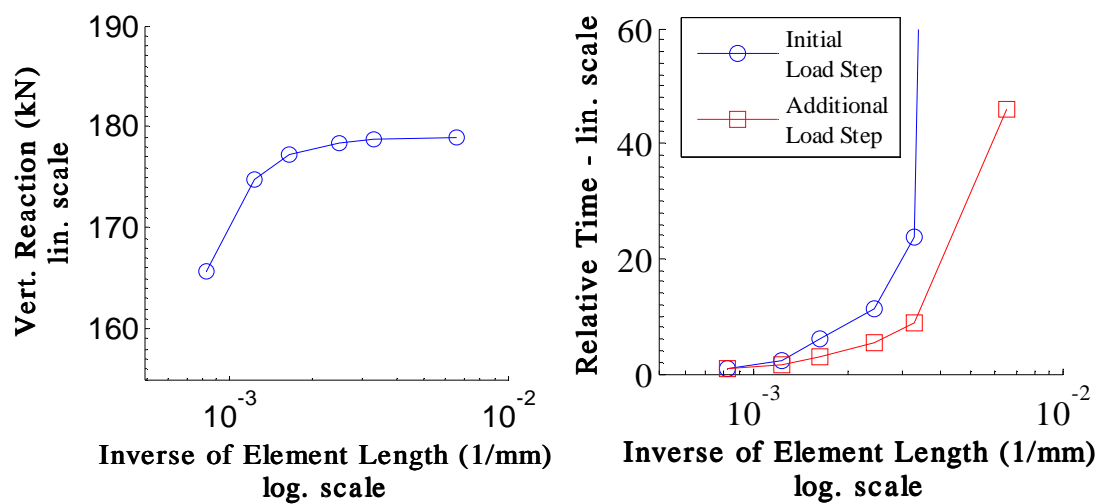


Fig. 2.7: Convergence of the summed reaction of bridge girders.

Summary

A generalized 3-D FEA bridge model was created for use in *OpenSees* and was designed for the purpose of analyzing girder live-load distribution factors to assist in bridge rating. The bridge model characteristics are listed below for reference:

- The model is made up of shell elements for the deck, frame elements for the girders, and rigid beam links connecting these two element types.
- Using the Tcl scripting language, a loading procedure was created to simulate the live-load exerted by moving truck loads across the bridge deck in order to develop an adequate design envelope for analysis.
- The model exhibited adequate convergence to a specified support reaction at an element length less than 610 mm (24 in).

References

- American Association of State Highway and Transportation Officials (AASHTO). (2003). *LRFD bridge design specifications*, 2nd Ed. with Interims, Washington, D.C.
- Barr, P. J., Eberhard, M. O., and Stanton, J. F. (2001). "Live-load distribution factors in prestressed concrete girder bridges." *J. Bridge Eng.*, 6(5), 298-306.
- Barr, P. J., Woodward, C. B., Najera, B., and Amin, Md. N. (2006). "Long-term structural health monitoring of the San Ysidro bridge." *J. Performance Const. Facilities.*, 20(1), 14-20.
- Bathe, K.-J., Iosilevich, A., Chapelle, D. (2000). "An evaluation of the MITC shell elements." *Computers and Structures*, 75, 1-30.
- Chung, W., Sotelino, E. D. (2006), "Three-dimensional finite element modeling of composite girder bridges." *J. Eng. Structures.*, 28, 63-71.
- Hughs, E., and Idriss, R. (2006). "Live-Load Distribution Factors for Prestressed Concrete, spread box-girder bridge." *J. Bridge Eng.*, 11(5), 573-581.
- Mabsout, M., Tarhini, K. M., Jabakhang, T., and Awwad, E. (2004). "Wheel load distribution in simply supported concrete slab bridges." *J. Bridge Eng.*, 9(2), 147-155.
- Mazzoni, S., McKenna F., Scott, M. H., and Fenves, G. L. (2006) "Open System for Earthquake Engineering Simulation User Command-Language Manual." Version 1.7.3. *University of California, Berkeley, CA.*
<<http://opensees.berkeley.edu/OpenSees/manuals/usermanual/>>
- McKenna, F., Fenves, G. L., and Scott, M. H. (2000). "Open system for earthquake engineering simulation." <<http://opensees.berkeley.edu>>
- Potisuk, T., and Higgins, C., (2007). "Field testing and analysis of CRC deck girder bridges." *J. Bridge Eng.*, 12(1), 53-62.
- Tabsh, S. W., and Tabatabai, M. (2001). "Live load distribution in girder bridges subject to oversized trucks." *J. Bridge Eng.*, 6(1), 9-16.
- Zokaie, T. (2000). "AASHTO-LRFD live load distribution specifications." *J. Bridge Eng.*, 5(2), 131-138.

Zokaie, T., Osterkamp, T. A., and Imbsen, R. A. (1991). "Distribution of wheel loads on highway bridges." *Final Rep. Project No. 12-26/1*, National Cooperative Highway Research Program, Transportation Research Board, National Research Council, Washington, D.C.

Chapter 3: Validation of a Generalized 3-D Finite Element Bridge Model

Objective

In chapter two, a generalized three-dimensional finite element bridge model was created for use in *OpenSees*. It was created for accurate and efficient bridge rating with the determination of girder distribution factors in concrete bridges of regular geometry. Validation and testing of this model is necessary in order to assess its actual performance and capabilities and to determine the applicability of *OpenSees* to three-dimensional bridge modeling for live-loads. This is completed through a previous comparison study of bridges with a collection of field measured data to results from finite element modeling of these bridges.

Using the generalized model, the shear girder distribution factors for two individual bridges are evaluated at specific sections subject to the bridge instrumentation and finite element analyses of a previous study. After a comparison of the results, the bridges' overall controlling distribution factors are determined and compared to the specifications in AASHTO LRFD (2003).

Description of Bridges

The two bridges selected for this study were the Willamette River Bridge located near Newberg, Ore. on Highway 219, and the McKenzie River Bridge located in Lane County, Ore. on Interstate 5. The actual load distribution of these conventionally

reinforced concrete bridges was calculated with a collection of field test data and compared to a finite element analysis in Potisuk and Higgins (2007). Their regular geometry, combined with the availability of existing data for these bridges, makes them ideal for testing the validity of the generalized finite element model. Refer to Higgins et al. (2004) for the bridges' structural drawings.

The Willamette River Bridge consists of three equal length spans of 16.76 m (55 ft). The first span is simply supported and has five girders that are 368 mm (14.5 in) wide with an 1194 mm (47 in) depth. The following two spans make up a continuous section which consists of four girders with a 330 mm (13 in) width and 1194 mm (47 in) depth. These continuous spans are joined and supported by a 419 mm X 1727 mm (16.5 in X 68 in) bent cap above two 762 mm (30 in) square columns at the outer girder lines. The simply supported ends of this continuous section have 203 mm X 762 mm (8 in X 30 in) diaphragms. At the quarter points of each of the three spans, the diaphragms are 229 mm X 1143 mm (9 in X 45 in). The bridge is topped with a 152 mm (6 in) deck. Fig. 3.1 shows a plan view of the bridge layout and elevation views at the bent cap location of the continuous section.

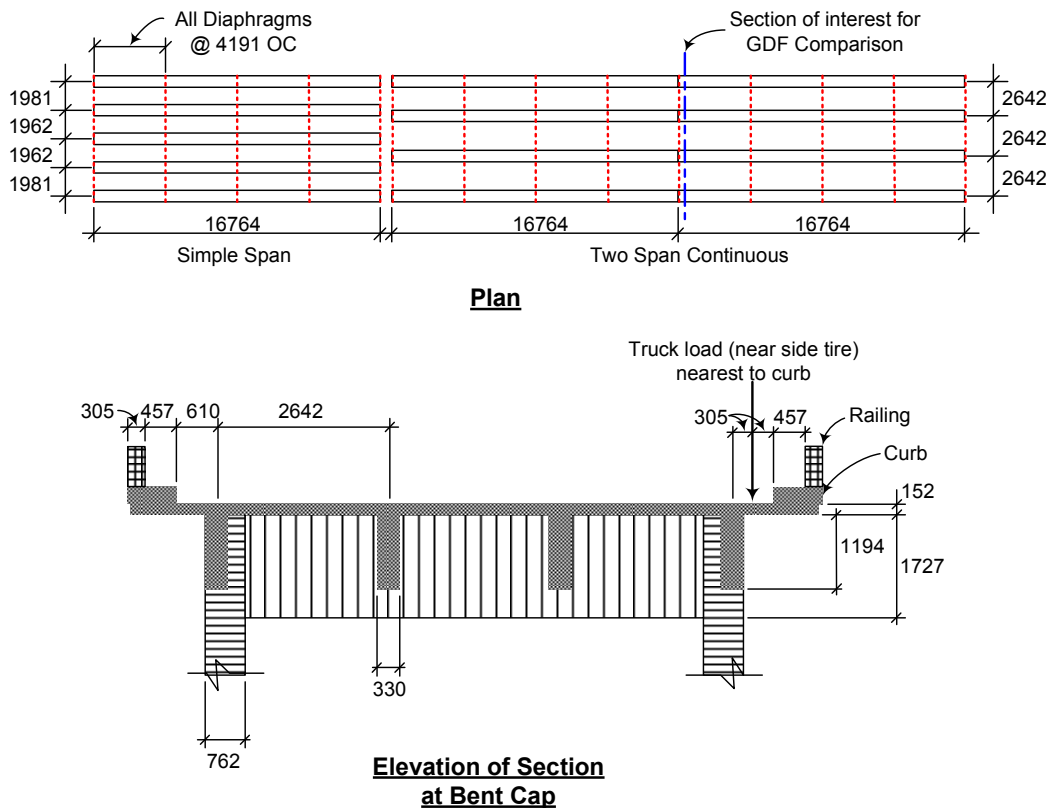


Fig. 3.1: Willamette River Bridge layout (all units in millimeters).

The McKenzie River Bridge is a four span bridge with one simply supported span and three continuous spans all with 15.24 m (50 ft) lengths. Like the Willamette River Bridge, diaphragms are located at quarter points of each of the four spans and are 229 mm X 1016 mm (9 in X 40 in). The simple span has four girders each with 330 mm X 1067 mm (13 in X 42 in) cross-sections. The four girders of the continuous spans have a depth of 1067 mm (42 in) and a width of 330 mm (13 in) near midspan but taper between the near diaphragms and continuous support locations to a 508 mm (20 in) width at the bent cap. The bent caps are 419 mm X 1753 mm (16.5 in X 69 in) and supported by 508 mm (20 in) square columns at the outer girder lines. The deck is 152

mm (6 in) thick. Fig. 3.2 shows a plan view of the bridge layout and elevation views at the bent cap location of the continuous section.

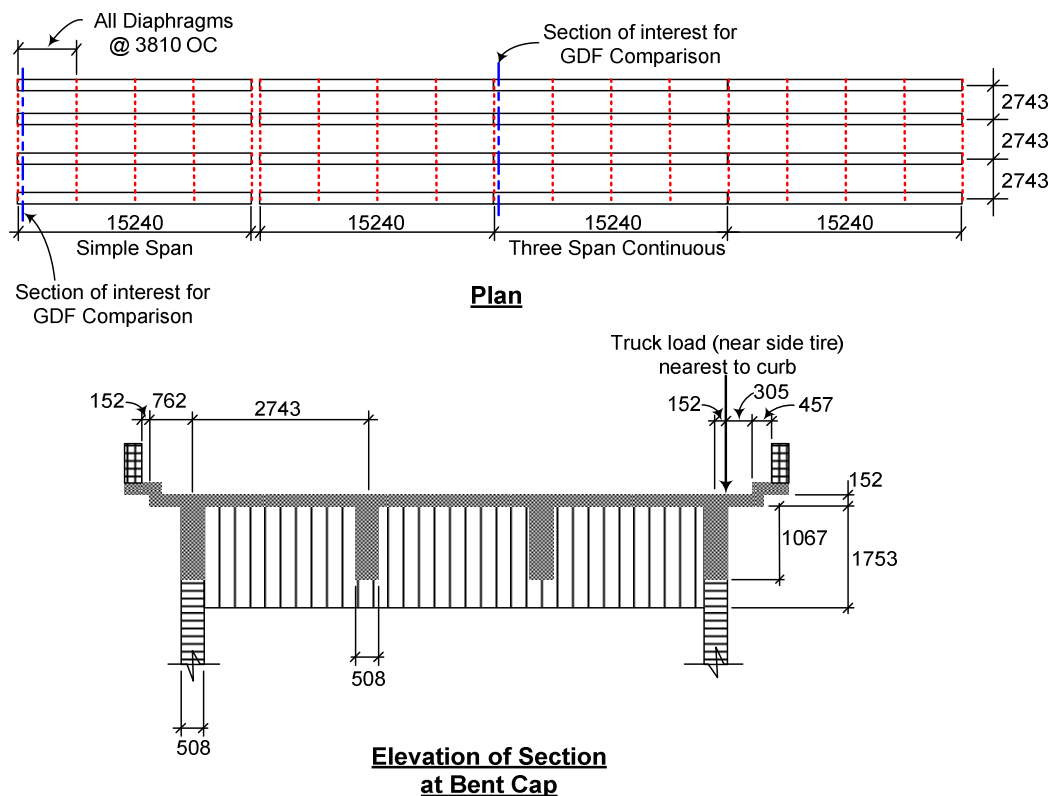


Fig. 3.2: McKenzie River Bridge layout (all units in millimeters).

Field Testing/Previous Analysis

Potisuk and Higgins (2007) give a full description of the field testing and bridge inspection procedure. In general, displacement transducers and strain gauges were installed at specific locations on the two bridges. The response was recorded for a passing truck at a creep speed of 8 km/hr (5 mi/hr) with known loads applied at discrete transverse locations. A compressive strength of 31.0 MPa (4500 psi) with a

standard deviation of 7.34 Mpa (1,065 psi) was recorded from concrete cores taken from the Willamette River Bridge. The elastic modulus was calculated as 26.4 GPa (3823 ksi); a Poisson's ratio of 0.2 was assumed. These material properties were used for all bridge analyses in Potisuk and Higgins (2007).

From the strain gauge data collected at the instrumented locations, shear distribution was determined for one and two lanes loaded based on the maximum strain response in a girder at a given section divided by the total strain response of all girders at that section. The distributions were determined for both interior and exterior girders. The effect of the test truck in various lanes was superimposed to develop the multiple lane loaded distributions and included multiple presence factors from the AASHTO LRFD (2003) specification. Shear distribution factors based on formulas from the same specification were also determined in the study.

A finite element model was developed to compare the different methods used for calculating distribution factors. As discussed in the second chapter, the model consisted of shell elements for the complete girder and deck assembly. The element size was set to 279 mm (11 in) in each direction. The comparative results of the controlling distribution factors from the Potisuk and Higgins (2007) study are summarized in Table 3.1, where it is noted that AASHTO LRFD (2003) results are more conservative for all cases.

Table 3.1: Summary of results from Potisuk & Higgins (2007).

Bridge Section		Distribution Factor		
		AASHTO LRFD	Field Data	P&H FE
Interior girder	McKenzie (contin.)	0.884	0.330	0.660
	McKenzie (simple)	0.884	Not Recorded	0.624
	Willamette (contin.)	0.861	0.540	0.734
Exterior girder	McKenzie (contin.)	0.900	0.830	0.814
	McKenzie (simple)	0.900	Not Recorded	0.812
	Willamette (contin.)	0.923	0.460	0.846

Model Setup

The generalized three-dimensional finite element bridge model developed in *OpenSees* was used to analyze the continuous section of the Willamette River Bridge and, separately, the simple span and continuous span sections of the McKenzie River Bridge. All three models ignored the added thickness of the curb and rail sections on the overhangs. The thickness of the overhangs remained consistent with that of the deck at 152 mm (6 in). The overhang length for the Willamette River Bridge was set to 1372 mm (54 in) from the centerline of the external girders. For the McKenzie River Bridge, assuming the curb and rail were negligible contributors to the structural system, the length was set to 762 mm (30 in). The slight taper in the girder widths was ignored for simplicity assuming it will not significantly affect the distribution of forces along the girder. All other bridge dimensions were input consistently with the bridge geometries given in the description of bridges section. See App. A for an example of the Tcl variable input of the continuous section of the Willamette River Bridge.

The element lengths were set at 305 mm (12 in). There were eight shell divisions between girders in the Willamette River Bridge model giving an element width of 318 mm (13 in); the overhangs were divided into four sections giving an element width of 343 mm (13.5 in). The Willamette River Bridge model consisted of 3584 shell elements and 664 beam elements. The shell elements for the McKenzie River Bridge overhangs were divided into three sections giving 381 mm (10 in) elements and the shells between the girders were divided into nine equal elements giving a width of 305 mm (12 in). The model of the continuous portion of the McKenzie River Bridge consisted of 5148 shell elements and 983 beam elements; the model of the simple span had 1716 shell and 343 beam elements. The girders for all models were vertically restrained at bridge abutments and all columns were assumed fixed at their foundations. Fig. 3.3 shows an *OpenSees* display of the finite element bridge models.

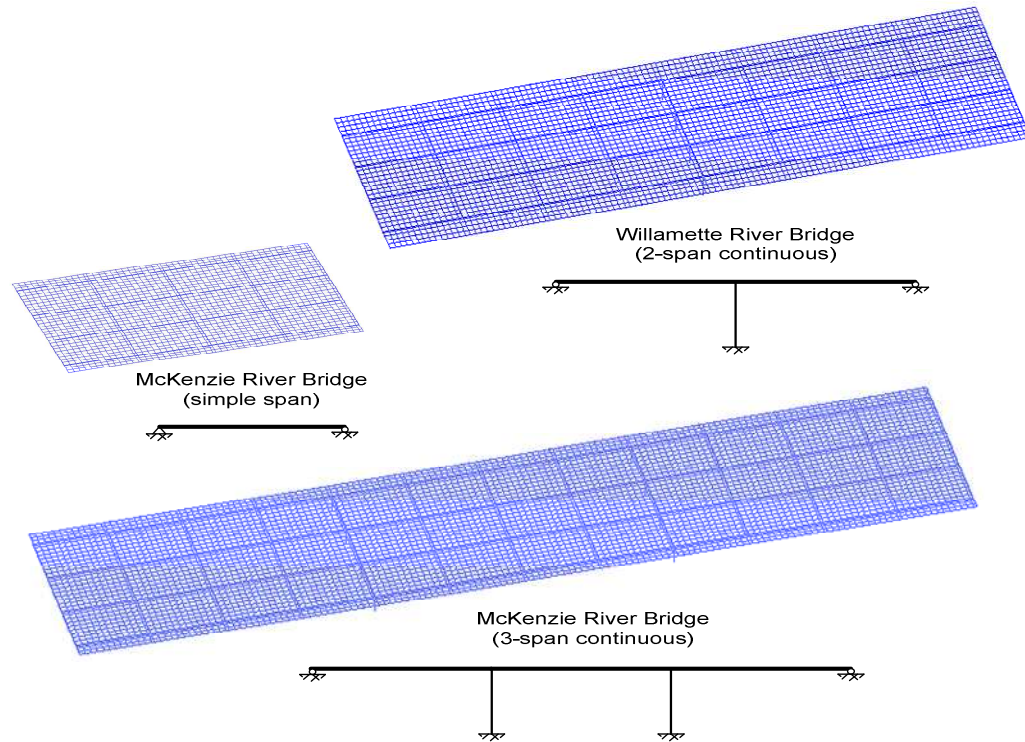


Fig. 3.3: FE bridge models with caption of applied boundary conditions.

Model Validation/Comparison

To compare the model to the results from Potisuk and Higgins (2007) and the AASHTO LRFD (2003) specifications, an HS-20 design truck was used for the analysis procedure with the distance between the rear axles set at the minimum value of 4.27 m (14 ft). Shear girder distribution factors were determined at the same locations of interest for both the interior and exterior girders of the bridge models. These longitudinal locations are distanced an effective depth away following the first encountered bent cap of the continuous sections and following the first abutment of the simple span section of the McKenzie River Bridge. The locations are noted previously in Fig. 3.1 and 3.2.

The truck loading procedure was selected in the generalized model and an HS-20 design truck was applied transversely across the selected longitudinal locations in order to determine the shear girder distribution factors. Cases for one lane loaded and two lanes loaded were considered separately. The equation for calculating distribution factors from the finite element analysis is shown as Eqn. 2.1 in the first chapter. This equation is used in Potisuk and Higgins (2007) and Tabsh and Tabatabai (2001). For readability it is again shown as

$$\text{GDF} = \frac{N \gamma f_m}{\sum_{i=1}^n f_i} \quad (\text{Equation 3.1})$$

where N=number of lanes loaded; γ =multiple presence factor (1.2 for N=1; 1.0 for N=2); f_m =maximum girder response (requisite response for shear or moment);

$\sum_{i=1}^n f_i$ =sum of response of all girders at the associated cross-section.

The transverse loading domain was bounded by a minimum distance of 305 mm (12 in) between the inside of the curbs and the nearside tire as shown in Fig. 3.1 and 3.2. This bound also considered a possible controlling distance of 610 mm (24 in) between the inside of the railings and the nearside tire load.

The shear girder distribution factors of the discrete locations, evaluated with the generalized model, closely match the previous results from Potisuk and Higgins (2007) and are shown in Table 3.2.

Table 3.2: Shear GDF comparison with Potisuk & Higgins (2007) FE analysis.

		Bridge Model	Distribution Factor		% Difference
			P&H FEM	FEM	
Exterior Girder	One lane loaded	McKenzie (contin.)	0.776	0.812	4.4%
		McKenzie (simple)	0.761	0.744	-2.3%
		Willamette (contin.)	0.842	0.802	-5.0%
	Two lanes loaded	McKenzie (contin.)	0.814	0.815	0.1%
		McKenzie (simple)	0.812	0.749	-8.4%
		Willamette (contin.)	0.832	0.839	0.8%
Interior Girder	One lane loaded	McKenzie (contin.)	0.491	0.574	14.5%
		McKenzie (simple)	0.553	0.575	3.8%
		Willamette (contin.)	0.461	0.528	12.7%
	Two lanes loaded	McKenzie (contin.)	0.660	0.698	5.4%
		McKenzie (simple)	0.624	0.712	12.4%
		Willamette (contin.)	0.734	0.660	-11.2%
				AVG	2.1%

Note: Bold indicates the controlling factor of each analysis for the interior and exterior

In most cases, the distribution factors of the generalized model with frame and shell elements are somewhat more conservative than those from the results of the complete shell model of Potisuk and Higgins (2007), especially for the interior girders. The difference between the interior and exterior girder distribution factors is likely due to considerations of the added curb thickness. This thickness was ignored for the analysis with the generalized model, but was included in the Potisuk and Higgins (2007) shell model. The added thickness of the curb would stiffen the exterior of the bridge cross-section and redistribute load from the interior to the exterior girders. The overall conservative results emphasize a stiffer model utilizing a combination of frame and shell elements as was noted in a comparison study in Barr and Amin (2006). In the study, they compared the girder reaction results from a full-scale slab-on-girder test

bridge to results from three different finite element models with the following modeling schemes: shells for the deck and frame elements for the girders, shell elements for the girders and deck, and solid elements for the deck with frame elements for the girders. The researchers noted that all models were within 4% of the measured and test data and the frame and shell model averaged slightly more conservative results.

Controlling Distribution Factors

The controlling girder distribution factors considering the entire bridge, as is required for bridge ratings, were sought for comparison to the results using distribution factor equations specified in the AASHTO LRFD (2003). The shear distribution factors were determined in Potisuk and Higgins (2007); to supplement, the controlling moment girder distribution factors were determined from LRFD section 4.6.2.2.2 combined with the factors previously equated from the lever rule and “pile cap” equations in Potisuk and Higgins (2007). The moment girder distribution equations for two lanes loaded in Table 4.6.2.2.2b-1 of AASHTO LRFD (2003) were found to control for the interior girders of both bridges; moment distribution factors for the exterior girders were controlled by the “pile cap” equation for the McKenzie River Bridge and by the lever rule for the Willamette River Bridge as was the case for the shear distribution factors.

All three bridge sections were analyzed again with the HS-20 design truck applied across the entire bridge at specified longitudinal and transverse increments in order to capture the maximum girder response. Different design trucks can be used at the analyst's discretion for a more in depth analysis of the maximum response, but the HS-20 design truck was used for all analyses for consistency. Also, applying loads across the entire area of these symmetric bridges is not always necessary; the analyst can apply the truck loads at discrete locations where the maximum response is anticipated. For this example, the truck loads were applied to the Willamette River Bridge in 141 longitudinal increments of 300 mm (11.8 in) for each of 21 horizontal increments of 335 mm (13.2 in) for one lane loaded and 183 mm (7.2 in) for two lanes loaded. The loading over the McKenzie River Bridge was divided into the same number and size of horizontal increments, but with the continuous portion divided into 191 longitudinal increments of 284 mm (11.2 in) and the simple section divided into 81 longitudinal increments of 297 mm (11.7 in). The total time for each of the analyses in the same order was 1002, 1975, and 299 seconds; the average time per applied load was 338, 492, and 176 milliseconds, respectively. The analyses are run on a *Dell* desktop computer with a 3.0 GHz *Intel Pentium 4* processor and 1.0 GB RAM on a *Windows XP* operating system.

The controlling shear girder distribution factors were recorded just past each continuous support and before the end abutment. The greatest distribution factors for the interior girders occurred near the abutment, but the controlling factors for the

exterior girders occurred after the first continuous support of both continuous bridge models as indicated in Table 3.3. The distribution factors for the positive moment were recorded at the center of each span. The first span of the Willamette River Bridge and the center span of the McKenzie River Bridge controlled with the highest resulting factors. Negative moment distribution factors were recorded over the continuous supports. The first support of the McKenzie River Bridge produced the greatest distribution factor. Single lane loaded and two lane loaded cases were considered with the application of appropriate multi-presence factors. The resulting girder distribution factors for shear and moment are summarized in Table 3.3.

Table 3.3: Generalized FEM girder distribution factors.

			Distribution Factor		
		Bridge Model	<i>Shear</i>	<i>Pos. Moment</i>	<i>Neg. Moment</i>
Exterior Girder	<i>One lane loaded</i>	McKenzie (contin.)	0.812*	0.624	0.880
		McKenzie (simple)	0.777	0.594	
		Willamette (contin.)	0.802*	0.586	0.866
	<i>Two lanes loaded</i>	McKenzie (contin.)	0.815*	0.768	0.980
		McKenzie (simple)	0.749	0.748	
		Willamette (contin.)	0.839*	0.747	0.978
Interior Girder	<i>One lane loaded</i>	McKenzie (contin.)	0.595	0.389	0.484
		McKenzie (simple)	0.587	0.390	
		Willamette (contin.)	0.572	0.381	0.459
	<i>Two lanes loaded</i>	McKenzie (contin.)	0.732	0.606	0.651
		McKenzie (simple)	0.723	0.603	
		Willamette (contin.)	0.710	0.587	0.606
Note: Bold indicates the controlling factor of each analysis for the interior and exterior					
* indicates value calculated at first interior support					

The controlling girder distribution factors from the results of the generalized bridge model are compared to the results from the AASHTO LRFD (2003) equations in Table 3.4. The factors determined with AASHTO LRFD (2003) are generally more conservative than those found with the generalized model except for the negative moment distribution of the exterior girder.

Table 3.4: Controlling girder distribution factor comparison.

		Bridge Model	Distribution Factor	
			AASHTO LRFD	FEM
Exterior Girder	<i>Shear</i>	McKenzie (contin.)	0.900	0.815
		McKenzie (simple)	0.900	0.777
		Willamette (contin.)	0.923	0.839
	<i>Positive Moment</i>	McKenzie (contin.)	0.900	0.768
		McKenzie (simple)	0.900	0.748
		Willamette (contin.)	0.923	0.747
	<i>Negative Moment</i>	McKenzie (contin.)	0.900	0.980
		McKenzie (simple)		
		Willamette (contin.)	0.923	0.978
Interior Girder	<i>Shear</i>	McKenzie (contin.)	0.884	0.732
		McKenzie (simple)	0.884	0.723
		Willamette (contin.)	0.861	0.710
	<i>Positive Moment</i>	McKenzie (contin.)	0.821	0.606
		McKenzie (simple)	0.821	0.603
		Willamette (contin.)	0.822	0.587
	<i>Negative Moment</i>	McKenzie (contin.)	0.821	0.651
		McKenzie (simple)		
		Willamette (contin.)	0.822	0.606

Summary

Shear girder distribution factors, computed from the generalized finite element model developed with *OpenSees*, were compared to results from the finite element procedure in Potisuk and Higgins (2007). Specific sections of the Willamette River Bridge and the McKenzie River Bridge were analyzed. This comparison study enabled a validation of the generalized bridge model and the use of *OpenSees* for further live-load analyses. The computed shear girder distribution factors matched closely, but were typically more conservative than the shell model of Potisuk and Higgins (2007). These results were consistent with the findings from previous research by Barr and Amin (2006) where it was found that complete shell models were slightly more flexible than frame and shell models and thus, more evenly distribute load across the bridge cross-section.

Following the model validation, both bridges were analyzed in order to compute the controlling girder distribution factors for both moment and shear. These distribution factors were compared to the factors determined with the AASHTO LRFD (2007) specification. The LRFD factors were much more conservative than those found with the generalized finite element bridge model in most cases. The distribution factors determined with the finite element model for the negative moment in the exterior girders were greater than the LRFD factors. Because of the generally conservative and the occasional un-conservative behavior of the AASHTO LRFD (2003) equations, a more refined analysis, such as with the finite element method, may be desired by the

bridge analyst in order to achieve a higher precision for bridge rating and a more economical design.

A considerable hindrance to employing the finite element method for a refined analysis is the time required to create and analyze individual bridge models. The efficiency of the generalized 3-D bridge model in terms of computational effort and model setup, combined with its reasonable accuracy, emphasizes the anticipated use of such a model – to efficiently and accurately rate bridges.

References

- American Association of State Highway and Transportation Officials (AASHTO). (2003). *LRFD bridge design specifications*, 2nd Ed. with Interims, Washington, D.C.
- Barr, P. J., and Amin MD. N. (2006) "Shear live-load distribution factors for I-girder bridges." *J. Bridge Eng.*, 11(2), 197-204.
- Higgins, C., et al. (2004). "Assessment methodology for diagonally cracked reinforced concrete deck girders." *Rep. No. FHWA-OR-RD-05-04*, Federal Highway Administration, Washington, D.C.
- McKenna, F., Fenves, G. L., and Scott, M. H. (2000). "Open system for earthquake engineering simulation." <<http://opensees.berkeley.edu>>
- Potisuk, T., and Higgins, C., (2007). "Field testing and analysis of CRC deck girder bridges." *J. Bridge Eng.*, 12(1), 53-62.
- Tabsh, S. W., and Tabatabai, M. (2001). "Live load distribution in girder bridges subject to oversized trucks." *J. Bridge Eng.*, 6(1), 9-16.
- Zokaie, T. (2000). "AASHTO-LRFD live load distribution specifications." *J. Bridge Eng.*, 5(2), 131-138.

Chapter 4: General Conclusions

The generalized three-dimensional finite element bridge model created for use in *OpenSees* was verified and comparatively validated for shear live-load girder distribution factors against previously studied conventionally reinforced concrete bridges. The model was also used to determine shear and moment distribution factors of the same bridges which were compared to those distribution factors calculated with the AASHTO LRFD (2003). The LRFD factors were found to be mostly conservative.

The efficiency of the generalized model in both bridge definition and analysis time combined with its accuracy makes it an appealing tool for use in analyzing a wide range of bridges of typical geometry in order to assess and rate them. The Tcl scripting language used with *OpenSees* enables a highly adaptable model defining all the geometric and material properties along with the loading procedure. These variables can be easily adjusted to suit the scope of the anticipated research.

To improve the range of applicability of the generalized model the following studies are suggested for future research:

- Validation of the model through analysis of skewed, variable width, and curved bridges
- Non-linear material and/or geometric properties for various loadings such as seismic, wind, and impact.

Appendices

Appendix A: Tcl Input for the Willamette River Bridge

```

# LOADING TYPE SELECTION
#-----
set Loading 1 ;# Select whether to use Truck Loading (Enter: 1) for GDFs or Point Loads
                (Enter: 2) for Influence Surface Plots
if {$Loading == 2} {
  set matlab [open InfLine.m w]
} elseif {$Loading == 1} {
  set matlab [open Bridgetemp3.m w]
}
puts $matlab "close all;"
puts $matlab "clear all;"

# Variables Defined by User
#-----
# Span Definition (input span lengths)
set Lspan {660.0 660.0} ;# Input consecutive span lengths (in)

set Nspan [length $Lspan] ;# Number of Spans

# Span Definitions (set element length)
set l 12.0 ;# Element length (longitudinal)(in) (include decimal to avoid
                integer division)
set sn 8 ;# Transverse shell divisions between girders
set Ng 4 ;# Number of girders

# Diaphragm Locations (Transvers Beams Connecting Girders)
# Enter as decimal of proportion of span (i.e. diaphragms at quarter points of span, 0.25)
set Xbeam {0.25 0.25} ;# Subsequent spans (enter 1.0 for no diaphragms)

# End Restraints
set fixity 1 ;# (1 – Pinned; 0 – End Cantilevers)

# Girder Spacing Definitions (Approach(X=0) and Exit(X=Ltot))
set Sa 104.0 ;# Approach Girder Spacing (in)
set S 104.0 ;# Girder Spacing (in)
set Sx 104.0 ;# Exit Girder Spacing (in)

# Skew Angle (Applicable only with Sa=Sx=S)
set skw 0.0 ;# Angle positive clockwise from Z-axis (degrees)

# Overhang Definition
set OH 54.0 ;# Deck overhang (in)
set sno 4 ;# transverse shell divisions on overhang

# Main Deck Definitions
set t 6.0 ;# Deck thickness (in)

```

Girder Dimensions

set b 13.0 ;# Width (in)
 set d 47.0 ;# Depth (in)

Diaphragm Dimensions

set bx 9.0 ;# Width (in)
 set dx 45.0 ;# Depth (in)

End Bent Cap Dimensions

set bce 9.0 ;# Width (in)
 set dce 30.0 ;# Depth (in)

Interior Bent Cap Dimensions

set bci 16.5 ;# Width (in)
 set dci 68.0 ;# Depth (in)

Material Section Properties

set E 3823.0 ;# Modulus girders (ksi)
 set Ed 3823.0 ;# Modulus deck (ksi)
 set nu 0.2 ;# Poisson's ratio deck
 set G [expr \$E/(2*(1+\$nu))] ;# Shear Modulus girders (ksi)

Column Locations and Properties

set Colloc {1 0 0 1} ;# (columns @ girder in order from Z=0, enter 1 for col. loc. @ girder, 0 for no col.; requires entry for all girders)
 set ColLint 442.0 ;# Length of Columns (in.)
 set Ec 3823.0 ;# Modulus of Columns (in.)
 set Icx 67500.0 ;# Moment of Inertia of cross-sect. (in4) (local axes consistent with global axes)
 set Icz 67500.0
 set Ac 900.0 ;# Area of cross-sect. (in2)

Loads

#-----
 # Truck Definition
 set axlwts {8.0 32.0 32.0} ;# Axle weights (k.)
 set axlspc {0.0 168.0 168.0} ;# Axle spacing (in.) (for multiple trucks in line, enter as additional axles)
 set axlwdth 72.0 ;# Tire width (in.)
 set TrkSp {} ;# Truck Spacing - Set distance between near truck tires of adjacent trucks (no entries for "one lane loaded")

Loading regions (Enter regions of interest. All Axles will pass through(all tires) X domain and remain within the Z domain)

Initial Load Location (front right tire headed from X>0)

set Xloc {0.1 1319.9 140.0} ;# X Loading Region (Enter: "first point" "last point" "number of divisions")

Initial Load Location (right tire starting from Z>0)

set Zloc {42.0 378.0 20.0} ;# Z Loading Region (Ignore truck width)(Enter: "first point" "last point" "divisions" NO REPEAT

